Residues in the H$^+$ Translocation Site Define the pK_a for Sugar Binding to LacY[†]

Irina Smirnova,[‡] Vladimir Kasho,[‡] Junichi Sugihara,[‡] Jun-Yong Choe,[‖] and H. Ronald Kaback*,[‡,§,⊥]

[‡]*Departments of Physiology and* [§]*Microbiology, Immunology, and Molecular Genetics, University of California Los Angeles, Los Angeles, California 90095-7327,* [‖]*Department of Biochemistry and Molecular Biology, Rosalind Franklin University of Medicine and Science, The Chicago Medical School, North Chicago, Illinois 60064, and* [⊥]*Molecular Biology Institute, University of California Los Angeles, Los Angeles, California 90095-7327*

ABSTRACT: A remarkably high pK_a of approximately 10.5 has been determined for sugar-binding affinity to the lactose permease of *Escherichia coli* (LacY), indicating that, under physiological conditions, substrate binds to fully protonated LacY. We have now systematically tested site-directed replacements for the residues involved in sugar binding, as well as H$^+$ translocation and coupling, in order to determine which residues may be responsible for this alkaline pK_a. Mutations in the sugar-binding site (Glu126, Trp151, Glu269) markedly decrease affinity for sugar but do not alter the pK_a for binding. In contrast, replacements for residues involved in H$^+$ translocation (Arg302, Tyr236, His322, Asp240, Glu325, Lys319) exhibit pK_a values for sugar binding that are either shifted toward neutral pH or independent of pH. Values for the apparent dissociation constant for sugar binding (K_d^{app}) increase greatly for all mutants except neutral replacements for Glu325 or Lys319, which are characterized by remarkably high affinity sugar binding (i.e., low K_d^{app}) from pH 5.5 to pH 11. The pH dependence of the on- and off-rate constants for sugar binding measured directly by stopped-flow fluorometry implicates k_{off} as a major factor for the affinity change at alkaline pH and confirms the effects of pH on K_d^{app} inferred from steady-state fluorometry. These results indicate that the high pK_a for sugar binding by wild-type LacY cannot be ascribed to any single amino acid residue but appears to reside within a complex of residues involved in H$^+$ translocation. There is structural evidence for water bound in this complex, and the water could be the site of protonation responsible for the pH dependence of sugar binding.

The lactose permease of *Escherichia coli* (LacY)[1] is a member of the major facilitator superfamily (MFS) of membrane transport proteins (*1*, *2*) that can utilize the free energy of an electrochemical H$^+$ gradient ($\triangle\tilde{u}_{H^+}$) to drive uphill accumulation of galactopyranosides (*3*–*9*). Alternatively, downhill transport of sugar can drive uphill transport of H$^+$ with generation of $\triangle\tilde{u}_{H^+}$, the polarity of which depends on the direction of the sugar concentration gradient (*10*, *11*). Sugar/H$^+$ symport is tightly coupled with a stoichiometry approximating unity (*4*, *12*, *13*). Cys-scanning and site-directed mutagenesis has shown that a relatively small number of amino acid side chains are irreplaceable with respect to active transport (*14*). Thus, Glu126 (helix IV), Arg144 (helix V), Glu269 (helix VIII), Arg302 (helix IX), His322, and Glu325 (helix X) have been implicated as key participants in substrate binding and/or H$^+$ translocation (*7*). Trp151 (helix V) is also critically involved in sugar binding, undergoing aromatic stacking with the galactopyranoside ring and also H-bonding with Glu269 (*15*, *16*).

Glu126, Arg144, Trp151, and Glu269 form the galactopyranoside-binding/recognition site (*17*–*19*), which is located in the

middle of the molecule and at the apex of a large hydrophilic cavity open to the cytoplasm (Figure 1A,B, green sticks). H$^+$ translocation involves residues primarily in the C-terminal six-helix bundle, which are positioned across the cavity from the sugar-binding site (Figure 1A,B, cyan sticks). Arg302 (helix IX), His322 (helix X), Tyr236 (helix VII), Glu325 (helix X), Asp240 (helix VII), and Lys319 (helix X) form a H-bond/salt bridge network between helices VII, IX, and X (Figure 1C). Arg302, Tyr236, His322, and Asp240 are within 3 Å of each other, and Glu325 and Lys319 flank the network from the cytoplasmic and periplasmic sides, respectively. A charge pair between Asp237 and Lys358 connects helices VII and XI and is important for membrane insertion and stability of LacY but not for sugar/H$^+$ symport (*20*–*22*).

LacY is a highly dynamic transport protein in which the sugar and H$^+$ binding sites become alternatively accessible to the periplasmic and the cytoplasmic sides of the membrane (*9*, *23*–*27*). Despite the availability of high-resolution, three-dimensional structures of LacY and a wealth of biochemical data, the mechanism of the coupling of sugar transport to H$^+$ translocation and of H$^+$ translocation itself remains unclear.

The finding that LacY affinity for galactopyranosides decreases at the alkaline pH (*28*, *29*) with a pK_a of about 10.5 (*30*) and numerous other observations (reviewed in refs *7* and *9*) indicate that protonation of LacY is required for sugar binding. Because the K_d^{app} remains constant from pH 5.5 to pH 9.0, it follows that under physiological conditions LacY is fully protonated with respect to sugar binding. Although amino acid side chains with alkaline pK_as such as those of Arg, Lys, or Tyr could be responsible for the high pK_a of binding, a hydrophobic

---

[1]Abbreviations: LacY, lactose/H$^+$ symporter from *Escherichia coli*; WT, wild type; DDM, dodecyl β-D-maltopyranoside; TDG, β-D-galactopyranosyl-1-thio-β-D-galactopyranoside; NPG, 4-nitrophenyl α-D-galactopyranoside; MIANS, 2-(4′-maleimidylanilino)naphthalene-6-sulfonic acid sodium salt; DACM, *N*-(7-dimethylamino-4-methylcoumarin-3-yl)maleimide; K_d^{app}, apparent dissociation constant; Trp→NPG FRET, Förster resonance energy transfer from Trp to NPG; $\triangle\tilde{u}_{H^+}$, electrochemical H$^+$ gradient.
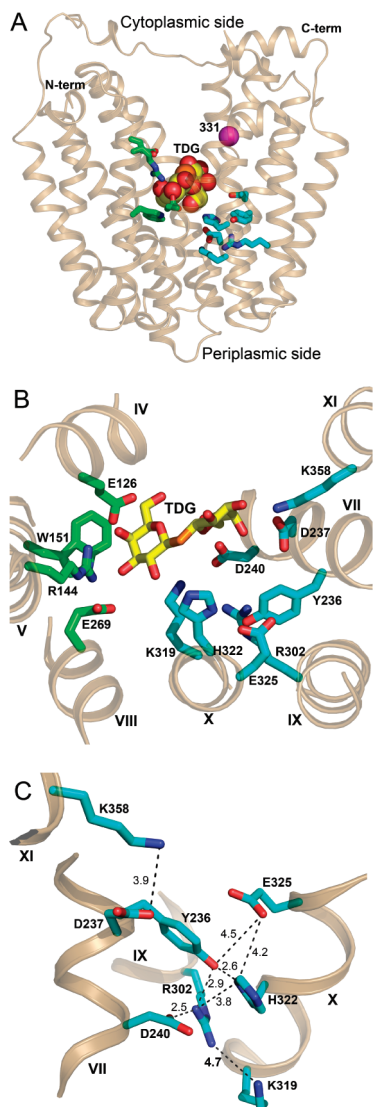
Published on Web 08/18/2009

FIGURE 1: X-ray structure model of LacY. (A) Side view of overall structure (PDB ID 1PV7) with TDG molecule (shown as spheres) bound at the apex of the cytoplasmic cavity. Amino acid residues implicated in sugar binding and H^+ translocation are shown as green or cyan sticks, respectively. The Cα atom at position 331, where the Cys residue introduced was labeled with fluorophore, is shown as a magenta sphere. (B) Cytoplasmic view from panel A showing part of the inner cavity with amino acid residues selected for mutational analysis and a TDG molecule shown as sticks. Transmembrane domains are labeled with Roman numbers. (C) Side view from the cytoplasmic cavity toward the proton translocation site (PDB ID 2CFQ). The network of hydrogen bond/salt bridge interactions is shown with only the shortest distances displayed as dashed lines (in Å). The structures are presented using Pymol 0.97 (DeLano Scientific, LLC).

environment, as well as clustering of amino acyl side chains, can markedly alter the pK_as of ionizable groups in proteins (*31, 32*).

Here we describe the effects of mutations in residues involved in sugar binding and/or H^+ translocation on the pK_a for sugar binding. Since replacement of essential side chains can dramatically decrease sugar affinity (*29, 33*), a highly sensitive fluorometric assay based on galactopyranoside-specific conformational change(s) was used to measure K_d^{app} for galactosides (*30*). Kinetic parameters of sugar binding were also determined directly by Trp to *p*-nitrophenyl α-D-galactopyranoside Förster resonance energy transfer (Trp→NPG FRET) combined with stopped flow (*34*). The pH dependence of the forward and reverse

rate constants indicates that the reverse rate constant (k_{off}) is a major determinant of the affinity change at alkaline pH. The findings demonstrate that the high pK_a observed for sugar binding is not related to the pK_a of a single amino acid side chain. We suggest that structural water coordinated within the H-bond/salt bridge network in the C-terminal six-helix bundle of LacY may participate in H^+ translocation as hydronium ion intermediate(s).

MATERIALS AND METHODS

Materials. Oligonucleotides were synthesized by Integrated DNA Technologies, Inc. (Coralville, IA). Restriction enzymes were purchased from New England Biolabs (Beverly, MA). The QuickChange II kit was from Stratagene (La Jolla, CA), and β-D-galactopyranosyl-1-thio-β-D-galactopyranoside (TDG) and 4-nitrophenyl α-D-galactopyranoside (NPG) were purchased from Sigma (St. Louis, MO). Fluorophores [2-(4′-maleimidylanilino)-naphthalene-6-sulfonic acid (MIANS) and *N*-(7-dimethylamino-4-methylcoumarin-3-yl)maleimide (DACM)] were obtained from Molecular Probes/Invitrogen (Eugene, OR) and from Anaspec (San Jose, CA). Dodecyl β-D-maltopyranoside (DDM) was obtained from Anatrace (Maumee, OH). Talon superflow resin was purchased from BD Clontech (Palo Alto, CA). All other materials were of reagent grade obtained from commercial sources.

Construction of Mutants and Purification of LacY. Construction of mutants, expression in *E. coli*, and purification of LacY were performed as described (*26*). All mutants contained an additional Cys residue (V331C in helix X) for labeling with maleimide-based fluorophores (MIANS or DACM) and a C-terminal 6-His tag that was used for affinity purification with a Talon resin. Purified proteins (10−15 mg/mL) in 50 mM sodium phosphate (NaP_i; pH 7.5)/0.02% DDM were frozen in liquid nitrogen and stored at −80 °C until use.

Labeling with Fluorophores. Purified LacY mutants (40−50 μM) were labeled at Cys331 with an equimolar concentration of fluorophore in 50 mM NaP_i (pH 7.0)/0.02% DDM in the presence of 15 mM TDG in order to protect Cys148 against alkylation as described (*30*). Control experiments with wild-type LacY exhibited essentially no labeling by MIANS under the same conditions.

Fluorescence Measurements. Steady-state fluorescence was monitored at room temperature using an SLM-Aminco 8100 spectrofluorometer (Urbana, IL) modified by OLIS, Inc. (Bogart, GA), and on a SPEX Fluorolog 3 spectrofluorometer (Edison, NY) as described (*30*) with excitation and emission wavelengths, respectively, of 330 and 415 nm for MIANS or 397 and 440 nm for DACM. Titrations were recorded after sequential addition of 5−10 μL of concentrated TDG to 2 mL of protein solution (0.4 μM) in 0.02% DDM/50 mM buffers with overlapping pH ranges. The buffers used were citrate-P_i (pH 5.5−6.5), NaP_i (pH 6.5−8.0), *N*-(1,1-dimethyl-2-hydroxyethyl)-3-amino-2-hydroxypropanesulfonic acid (AMPSO) (pH 8.0−9.5), and 3-(cyclohexylamino)-1-propanesulfonic acid (CAPS) (pH 9.5−11.0). Titration data were corrected for dilution and fluorescence drift at high pH. Data fitting was carried out by using SigmaPlot 10 (Systat Software Inc., Richmond, CA).

Stopped-flow measurements of Trp→NPG FRET were performed at 25 °C using an SLM-Aminco 8100 spectrofluorometer (Urbana, IL) modified with a USA stopped-flow unit (OLIS, Inc., Bogart, GA) as described (*34*). Protein concentrations were
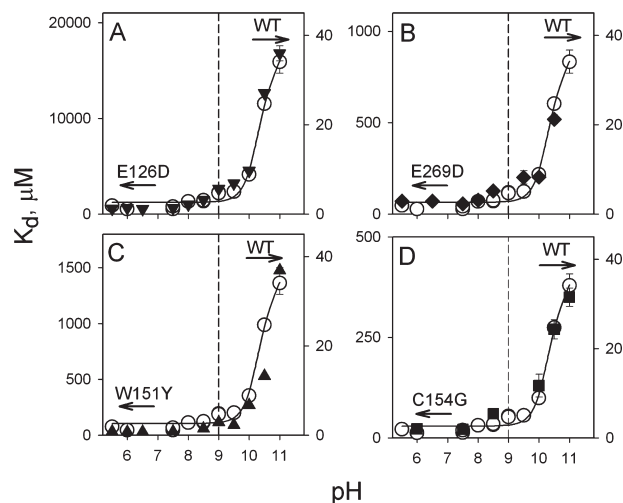
FIGURE 2: Effect of pH on K_d^{app} for TDG binding to MIANS-labeled V331C LacY with replacements of side chains in the vicinity of the sugar-binding site. Purified proteins (0.4 μM) were titrated with TDG at the indicated pH as described in Materials and Methods. The titrations are presented in Supporting Information Figure 11. Estimated K_d^{app} values are plotted versus pH and shown together with wild-type LacY data for comparison. The pK_a value for wild-type LacY (10.5) is estimated from hyperbolic fit of K_d^{app} dependency on H$^+$ concentration (solid line) (30). Vertical axes are as follows: on the right side for the wild-type LacY (○) and on the left side for the mutants (see arrows). The scales are proportional to the TDG affinity measured at pH 6.0 (see Table 1). (A) E126D (▼); (B) E269D (◆); (C) W151Y (▲); (D) C154G (■). The dashed vertical line marks pH 9.0.

0.5–2 μM. The same buffers were used as described for steady-state measurements. Typically, protein preincubated at an indicated NPG concentration was rapidly mixed with saturating concentrations of TDG (10–20 mM after mixing). Six to twelve stopped-flow traces were recorded for each data point, averaged, and fitted with a single exponential equation with the built-in Olis Globalworks software package or with SigmaPlot 10 (Systat Software Inc., Richmond, CA).

Transport Assays. Lactose accumulation by *E. coli* T184 expressing wild-type LacY or given mutants was performed as described (35).

Refinement of LacY Structure (*PDB ID 2cfq*). The best available structure of C154G LacY was used in a search for the presence of structural water molecules (see Supporting Information Refinement of LacY Structure for details). The refinement included all data in the resolution range from 2.81 to 9.99 Å without σ cutoff (28407 reflections) available from the deposited structure factor file (2cfq-sf.cif).

RESULTS

The pK_a for TDG Binding Does Not Change with Mutations in Residues Directly Involved in Sugar Binding. As shown previously (30), MIANS-labeled wild-type LacY binds TDG with a K_d^{app} near 1 μM in the pH range 5.5–8.0; the K_d^{app} is about 5-fold greater at pH 9.5 and 30-fold greater at pH 11.0 (Figure 2; Table 1). Although DACM-labeled LacY exhibits lower affinity (i.e., higher K_d^{app}), a similar dependence on pH is observed (Table 1).

Residues Glu126, Arg144, Trp151, and Glu269 participate directly in sugar binding (Figure 1B, green sticks), and mutation of each drastically decreases TDG-binding affinity (Figure 2, y axes; Table 1; see also Supporting Information Figure 11). Mutations E126A or E126Q completely abolish sugar binding

Table 1: TDG Binding Affinity (K_d^{app} Values) for LacY Mutants at Different pH and Estimated pK_a Values

V331C/LacY mutant[a]	TDG binding,[b] K_d (μM)					K_d vs pH pK_a
	pH 6.0	pH 7.5	pH 9.5	pH 10.5	pH 11.0	
WT[c]	1.1	1.2	5.0	25	34	~10.5
WT (DACM)	21	20	60	160	310	
C154G	22	21	160	270	350	~10.5
E126D	540	620	3200	12630	16780	~10.5
W151Y	30	33	92	530	1480	~10.5
E269D	70	75	200	520		~10.5
R302K	26	95	220	240	290	8.4
R302A	16	60				nd
R302A (DACM)	62	122	199	210	230	
Y236A	55	110	356	390		8.0
Y236C	57	78	337	430		8.7
Y236T	53	81	382	520	540	8.9
Y236S	75	146	371	580	600	8.1
Y236N	13	25	302	390		9.1
Y236K	230	305	287	336		nd
Y236F	100	190	188	228		nd
Y236W	407	784	2290	2297	2750	8.2
H322A	130	266	477	885	1440	nd
H322N	170	458	850	1060	1960	nd
H322N/154G	1100	1200	3000	3400		nd
H322Q	339	967	1100	2464	4180	nd
H322K	254	300	815	1956	3420	nd
H322F	202	350	257	260		nd
H322R	607	715	1238	2800		nd
H322Y	265	520	598	760	850	nd
D240E	12	20	223	595	1050	~10.5
D240A	66	55	104	280	580	nd
D240N	200	140	200	360	380	nd
K319R	2	2	3	25		~10.5
K319L	1.5	1.2	2.1	2.8	5.5	nd
K319Q	4.3	5	6.6	27	33	nd
E325D	11	16	350	870	1965	~10.5
E325A	2.1	3.1	6.1	4.5	6.5	nd
E325Q	0.7	0.8	1.1	1.1	0.9	nd
E325Q (DACM)	8.2	8.6	11.8	12	15	

[a]All mutants are labeled with MIANS (not indicated) or with DACM (as indicated in parentheses). [b]K_d^{app} are estimated from titration data shown in Supporting Information Figures 11–15; there is no detectable TDG binding to E126Q or A, to R144K or A, to H322M, and to E269Q, A, N, H, K, Y, or G; pK_a values are estimated for the pH range 5.5–11 as shown on Supporting Information Figure 16. [c]Data for wild-type LacY were published before (30).

and transport (36, 37), thereby precluding studies on the effect of pH. The conservative mutant E126D exhibits a K_d^{app} increased more than 500-fold (Table 1); nevertheless, the pH dependence of sugar binding remains unchanged (Figure 2A; Table 1). Only the conservative replacement of Glu269 with Asp maintains activity; the mutants E269A, Q, N, H, K, G, and Y exhibit no sugar binding (data not shown). Although the mutant E269D exhibits a pK_a similar to that of wild type, affinity for TDG decreases about 70 times relative to wild type (Figure 2B; Table 1). The observation is consistent with other evidence (38, 39) indicating that Glu269 may directly interact with the galactopyranosyl ring.

Trp151 is important for correctly orienting bound galacto-pyranosides, and even relatively conservative replacements with Tyr or Phe decrease sugar affinity about 20 or 50 times, respectively (15). Sugar binding by MIANS-labeled mutant W151Y exhibits a pH dependence profile similar to wild-type LacY with a K_d^{app} that is about 30 times higher (Figure 2C;
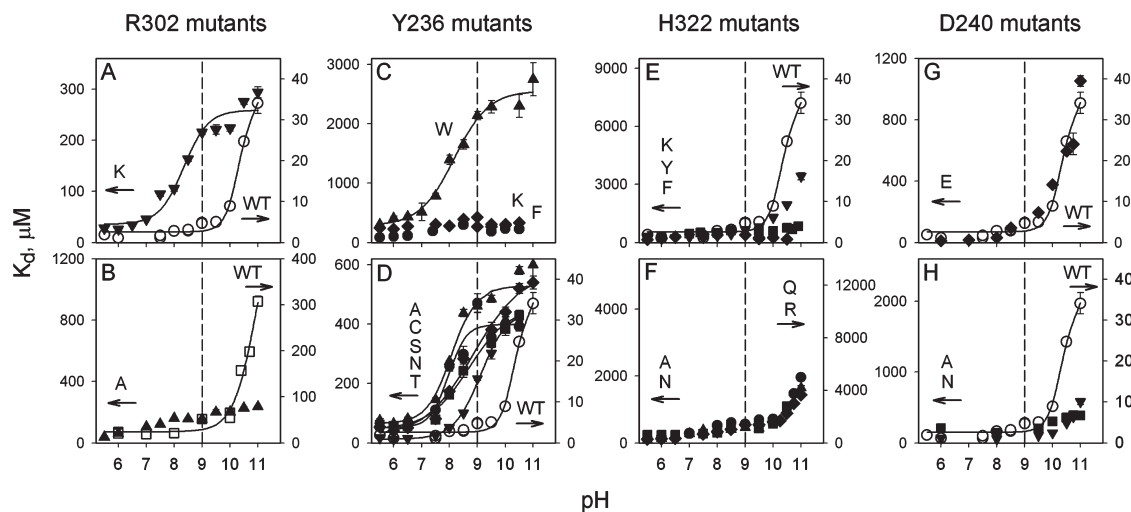
FIGURE 3: Effect of pH on K_d^{app} for TDG binding to the LacY mutants with replacements in H^+ translocation site at positions of Arg302, Tyr236, His322, and Asp240. Data for mutated residues (marked on the top) are presented on upper and lower panels. Side chain replacements are shown on each panel as single letters together with arrows indicating the vertical axes for K_d^{app} values. Titrations were carried out as described in Materials and Methods and in Figure 2 (see also Supporting Information Figures 12–14). Data for wild-type LacY (open symbols) are shown for comparison. MIANS-labeled V331C LacY was used in all experiments except R302A that was labeled with DACM and compared to DACM-labeled wild type (panel B). Vertical scales are proportional to K_d^{app} at pH 6 for wild-type LacY (see Table 1). (A) R302K (▼); (B) DACM-labeled R302A (▲); (C) Y236F (●), Y236K (◆), Y236W (▲); (D) Y236A (●), Y236C (■), Y236S (▲), Y236N (▼), Y236T (◆); (E) H322K (▼), H322Y (■), H322F (◆); (F) H322N (●), H322A (◆), H322Q (▲), H322R (■); (G) D240E (◆); (H) D240A (▼), D240N (■). pK_a values are estimated from hyperbolic fit of K_d^{app} dependency on H^+ concentration (solid lines) as shown in Supporting Information Figure 16 and presented in Table 1.

Table 1). Cys154 is located one turn of helix V from Trp151 toward the periplasmic side, and mutant C154G binds sugar but does almost negligible transport because it is paralyzed on the periplasmic side (25, 26, 40–42). The pH dependence of sugar binding for the C154G mutant is also similar to WT LacY, with an increase in K_d^{app} of about 20-fold (Figure 2D).

Arg144, which likely forms a bidentate H-bond with the 3- and 4-OH groups in the galactopyranoside ring (17), is strictly conserved in related symporters (43). Even replacement with Lys leads to complete loss of sugar binding (36, 37). Therefore, replacements for Arg144 were precluded from this study.

Mutations That Decrease TDG Affinity and Change the pK_a for Binding. Arg302, Tyr236, His322, and Asp240 form an H-bond/salt bridge cluster in the middle of the C-terminal six-helix bundle (Figure 1C, cyan sticks), and any single replacement results in a marked decrease in the affinity for sugar and also a concomitant change in the pH dependence of K_d^{app} (Figure 3; Table 1; see also Supporting Information Figures 12–14). Two distinct effects on the pH profiles are observed: (i) a significant shift of pH dependence toward lower pK_a values, or (ii) suppression of the effect of alkaline pH on sugar affinity. An acid shift of 1.5–2.5 pH units is observed for mutant R302K (Figure 3A; Table 1) and for all Tyr236 mutants, except Y236F and Y236K (Figure 3C,D; Table 1). K_d^{app} values increase sharply between pH 7.5 and pH 9.5 and approach a plateau with at least a 10-fold decrease in TDG affinity in each mutant. The other effect, suppression of the increase in K_d^{app} at alkaline pH, is observed with mutant R302A (Figure 3B; Table 1) and for mutants D240N or D240A (Figure 3H; Table 1), as well as for all the His322 replacements (H322K, Y, F, A, N, Q, R; Figure 3E,F; Table 1) and mutants Y236F or Y236K (Figure 3C; Table 1). The only conservative replacement in this group, mutant D240E, does not exhibit a change in pK_a relative to wild-type LacY (Figure 3G; Table 1). However, sugar affinity in all of these mutants, particularly the replacements for His322, is drastically decreased (Table 1; Figure 3, y axes).

High-Affinity Sugar Binding Independent of pH Is Observed with Neutral Replacements for Lys319 or Glu325. The most striking effect of mutations is found when Lys319 or Glu325 is replaced with neutral residues in the mutants K319L, K319Q, E325A, and E325Q (Figure 4; Table 1; see also Supporting Information Figure 15). The affinities are similar to those observed for wild-type LacY at pH 6–8 and remain high (i.e., low K_d^{app}) over the entire pH range from 5.5 to 11. Mutant E325Q was also tested with DACM-labeled V331C LacY (Figure 4C) with the same result: the high-affinity TDG binding is independent of pH. It is remarkable that elimination of an ionizable side chain at position 319 or 325 results in high-affinity TDG binding even at extremely low H^+ concentrations.

The affinity for TDG does not change significantly with the mutant K319R (Figure 4A; Table 1) but decreases markedly with the mutant E325D (Figure 4B; Table 1), and both mutants exhibit essentially the same pH dependence as wild-type LacY. These observations are consistent with the notion that neutral replacements of Glu325 and Lys319 completely block transport with little effect on sugar binding, but the protein with conservative replacements at these positions retains at least partial transport activity (29, 35, 44–49) (see also Supporting Information Figure 17).

Effect of pH on Pre-Steady-State Kinetics of Direct Sugar Binding. Rates (k_{obs}) of TDG induced conformational change with MIANS-labeled LacY have been shown to increase at alkaline pH. The forward rate (k_{on}^{app}) does not depend on pH, while the reverse rate (k_{off}^{app}) is clearly pH dependent, resulting in an increase of K_d^{app} ($K_d = k_{off}/k_{on}$) at alkaline pH with pK_a of about 10.5 (30). Consistently, a similar effect of pH on the kinetic parameters is observed when sugar binding is measured directly by Trp→NPG FRET. Protein samples equilibrated with NPG were mixed rapidly with TDG at saturating concentrations, and reverse rate constants (k_{off}) were measured directly by recovery of Trp fluorescence after displacement of bound NPG with excess TDG (30, 34). Measurement of the reverse rates is convenient for
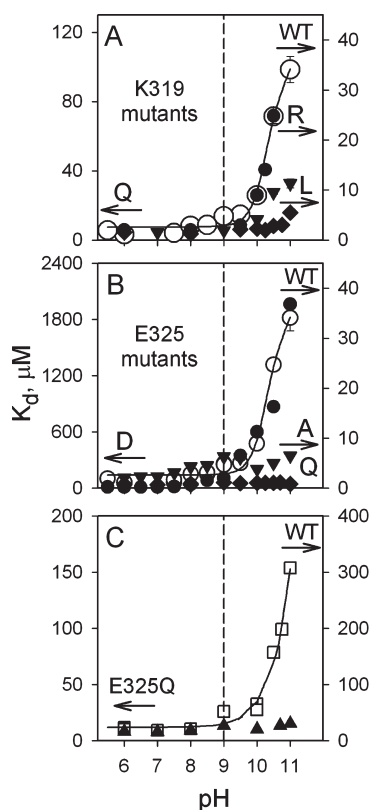
FIGURE 4: Effect of pH on K_d^{app} for TDG binding to the LacY mutants with replacements of Lys319 and Glu325. MIANS-labeled proteins were used in panels A and B; DACM-labeled E325Q and wild type were used in panel C. Data are analyzed and presented in Figures 2 and 3 (see also Table 1 and Supporting Information Figure 15). (A) K319R ($\bullet$), K319L ($\blacklozenge$), K319Q ($\blacktriangledown$); (B) E325D ($\bullet$), E325A ($\blacktriangledown$), E325Q ($\blacklozenge$); (C) DACM-labeled E325Q ($\blacktriangle$). Data for wild-type LacY (open symbols and solid lines) are shown for comparison.

testing the effect of pH since k_{off} is concentration independent and slower than k_{obs} ($k_{obs} = k_{off} + k_{on}[NPG]$). Stopped-flow traces recorded at given pH values and NPG concentrations for wild-type LacY and mutant K319L are shown in Figure 5. All traces are fitted with a single-exponential equation, which allows estimation of rates and amplitudes of the fluorescence change. The results demonstrate that (i) the rate of NPG displacement (k_{off}) is independent of NPG concentration with either wild-type LacY (Figure 5A; $k_{off} = 80 \pm 2$ s^{-1} for traces 1−4) or the K319L mutant (Figure 5B; $k_{off} = 70 \pm 5$ s^{-1} for traces 1−3), (ii) the amplitudes increase with NPG concentration for both the wild-type LacY (Figure 5A; amplitudes are 9%, 16%, 22%, 25% for 12, 50, 100, 300 μM NPG, respectively) and mutant K319L (Figure 5B; amplitudes are 9%, 26%, 33% for 5, 20, 100 μM NPG, respectively), and (iii) the displacement rate (k_{off}) increases at alkaline pH for wild-type LacY (Figure 5C; k_{off} values are 69 $\pm$ 2 s^{-1}, 79 $\pm$ 2 s^{-1}, 160 $\pm$ 7 s^{-1}, 224 $\pm$ 10 s^{-1} at pH 6.0, 9.0, 10.25, 10.5, respectively), while k_{off} hardly changes with mutant K319L (Figure 5D; k_{off} values are 54 $\pm$ 2 s^{-1}, 44 $\pm$ 4 s^{-1}, 69 $\pm$ 10 s^{-1} at pH 6.0, 9.0, 10.5, respectively).

The concentration dependence of the change in amplitudes with wild-type LacY shows that affinity for NPG decreases at alkaline pH. Thus, K_d values calculated from hyperbolic fits are 43 $\pm$ 5 μM, 30 $\pm$ 2 μM, and 320 $\pm$ 60 μM at pH 7.0, 9.0, and 10.25, respectively (Figure 6A). The pH dependencies of k_{off} as measured by stopped flow and k_{on} calculated from the K_d are presented in Figure 6D. Clearly, k_{on} is pH independent
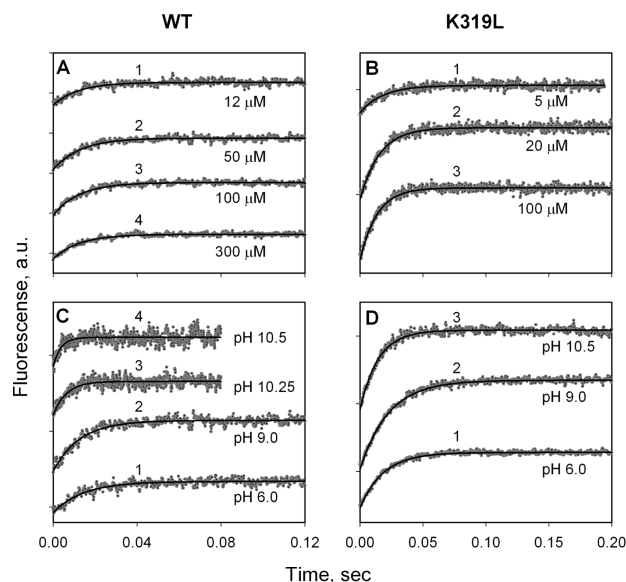

FIGURE 5: Stopped-flow traces of Trp fluorescence change showing displacement of bound NPG by the excess of TDG at various NPG concentrations and different pHs. Average of seven to nine individual traces (gray dots) are fitted with a single exponential equation (solid lines). Amplitudes are calculated as percentage of fluorescence change relative to the final level of fluorescence. (A) WT LacY at pH 9.0 and indicated NPG concentrations. Amplitudes of fluorescence change are 9%, 16%, 22%, and 25% for traces 1, 2, 3, and 4, respectively. Estimated k_{off} is 80 $\pm$ 2 s^{-1}. (B) K319L LacY at pH 10.5 and indicated NPG concentrations. Amplitudes of fluorescence change are 9%, 26%, and 33% for traces 1, 2, and 3, respectively. Estimated k_{off} is 70 $\pm$ 5 s^{-1}. (C) WT LacY, pH dependence of displacement rate. Estimated k_{off} values are 69 $\pm$ 2 s^{-1}, 79 $\pm$ 2 s^{-1}, 160 $\pm$ 7 s^{-1}, and 224 $\pm$ 10 s^{-1} for traces 1, 2, 3, and 4, respectively. (D) K319L LacY, pH dependence of displacement rate. Estimated k_{off} values are 54 $\pm$ 2 s^{-1}, 44 $\pm$ 4 s^{-1}, and 69 $\pm$ 10 s^{-1} for traces 1, 2, and 3, respectively. See Materials and Methods for details.
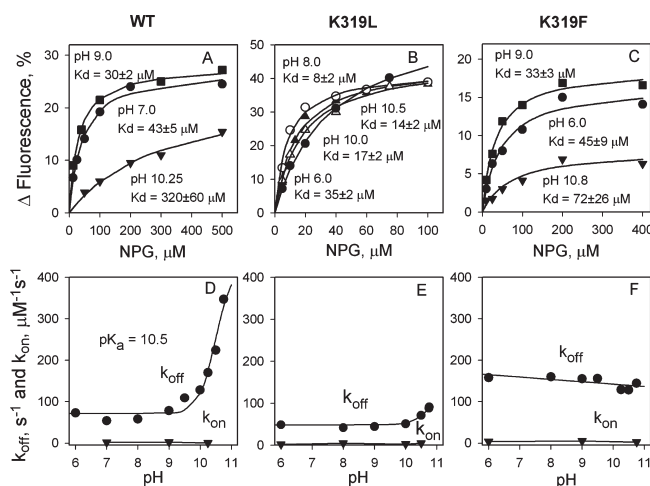

FIGURE 6: Kinetics of displacement of bound NPG by the excess of TDG; comparison of WT LacY with uncharged replacements for Lys319. Upper panels: Dependence of amplitude of fluorescence changes on NPG concentrations at different pH. Solid lines are hyperbolic fits to the data. Calculated K_d values at each pH are indicated. Lower panels: pH dependencies of measured displacement rates (k_{off}) and k_{on} calculated from K_d ($k_{on} = k_{off}/K_d$) are presented as circles and triangles, respectively.

(1.5 $\pm$ 0.9 $\times$ 10^6 M^{-1} s^{-1}), while k_{off} increases dramatically at alkaline pH with pK_a at about 10.5. The pH dependencies of the kinetic constants measured directly here for binding of NPG to unlabeled protein and reported earlier for TDG binding to
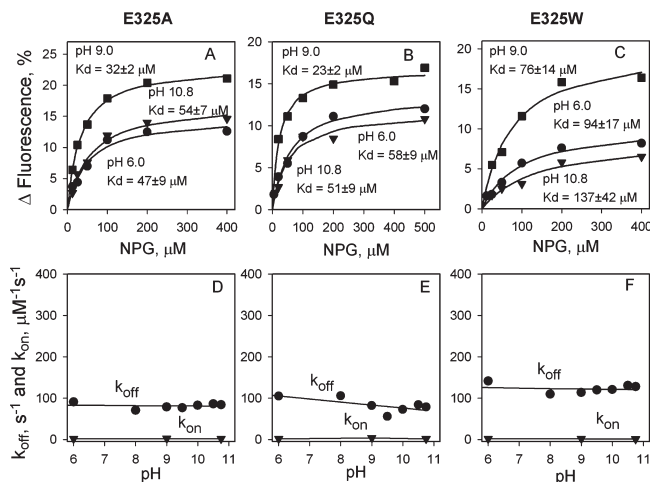
FIGURE 7: Kinetics of displacement of bound NPG by the excess of TDG for uncharged replacements of Glu325. Upper panels: Dependence of amplitude of fluorescence changes on NPG concentrations at different pHs. Solid lines are hyperbolic fits to the data. Calculated K_d values at each pH are indicated. Lower panels: pH dependencies of measured displacement rates (k_{off}) and k_{on} calculated from K_d are presented as circles and triangles, respectively.

MIANS-labeled LacY (*30*) are practically identical: the on-rate is pH independent, while the off-rate increases at alkaline pH with pK_a around 10.5. It follows that the pK_a of ~10.5 observed with wild-type LacY is an intrinsic property of the protein that reflects binding specifically and is not due to a conformational change or to labeling with fluorophores.

Neutral replacements for Lys319 or Glu325 practically abolish the effect of pH on the kinetic parameters for NPG binding. K_d values estimated from the effect of NPG concentration on fluorescence amplitude are similar to the K_d for wild-type LacY at neutral pH but do not change significantly at alkaline pH (Figure 6B,C; Figure 7A−C). Unlike with wild-type LacY, k_{off} is essentially unchanged in the pH range from 6 to 10.8 (compare Figure 6D with Figure 6E,F and Figure 7D−F). The displacement rate measured in each experiment represents a true value of k_{off} since it is not different from the k_{off} value obtained from the dependence of k_{obs} on NPG concentration (see Figure 8 for example). Calculated k_{on} values for all these mutants are also unaffected by pH. These data provide strong support for the remarkable conclusion that neutral replacements for Lys319 or Glu325 in LacY result in high-affinity sugar binding even at pH 11.

All replacements for amino acid side chains involved in the H-bond/salt bridge cluster (Arg302, Tyr236, His322, or Asp240) decrease sugar affinity (Table 1), thereby complicating pre-steady-state measurements. Nevertheless, the pH dependence of kinetic parameters for NPG binding was measured directly for R302A, D240E, and D240A mutants (Figure 9). The pH dependence of k_{off} for each mutant is very similar to the pH dependence of the K_d^{app} obtained with the corresponding MIANS-labeled protein. R302A and D240A demonstrate little change of k_{off} with pH, while E240E exhibits a sharp increase of the displacement rate in alkaline pH (compare Figure 9D−F, respectively, with Figure 3B, G,H). Clearly, the rate of sugar release (k_{off}) is a key parameter, which is primarily affected by the protonation state of the H-bond/salt bridge cluster that defines the pH dependence of the K_d^{app}.

DISCUSSION

LacY binds galactopyranosides specifically in a manner that is pH dependent (*28, 29*), and protonation is required for
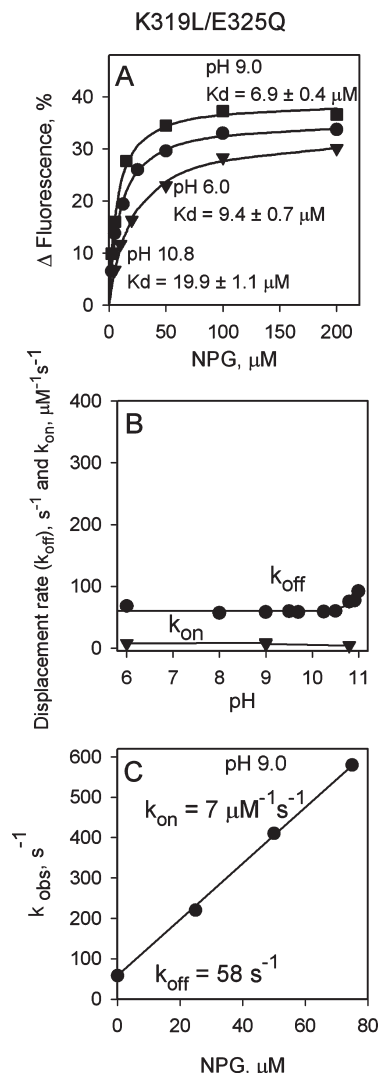

FIGURE 8: Kinetics of NPG binding to the LacY mutant K319L/E325Q. (A, B) Displacement of bound NPG by the excess of TDG. Measurements are carried out as in Figure 5−7. (A) NPG concentration dependence of amplitude of fluorescence change at pH 6.0 (●), 9.0 (■), and 10.8 (▼). Solid lines are hyperbolic fits to the data. Calculated K_d values at each pH are shown. (B) Dependence of the rates of fluorescence increase on pH. Measured k_{off} is 64 ± 8 s^{-1} in the pH range 6.0−10.8 (k_{off} at pH 9.0 is 58 s^{-1}). The k_{on} values ($6.5 \pm 2.4 \mu M^{-1}$ s^{-1}) are calculated from measured k_{off} and K_d. (C) Binding of NPG to the LacY mutant at pH 9.0 measured directly. Protein (0.5 μM) was rapidly mixed with NPG at the indicated concentrations, stopped-flow traces were recorded, and the rates of fluorescence decrease (k_{obs}) were estimated from exponential fits to the data. All given concentrations are final after mixing. NPG concentration dependence of k_{obs} is presented. Each point is an average of seven to nine measurements. The solid line is the linear fit to the data ($k_{obs} = k_{off} + k_{on}[NPG]$). The slope is k_{on} ($7 \mu M^{-1}$ s^{-1}) and the intercept with the y axis is k_{off} (58 s^{-1}). The k_{off} value for NPG measured directly is exactly the same as measured by displacement of bound NPG with the excess of TDG (panel B). The estimated K_d (8.3 μM) is in a good agreement with K_d measured by displacement (panel A).

high-affinity binding (reviewed in refs *7* and *9*). In addition, it has been shown recently (*30*) that various galactopyranosides bind to wild-type LacY with pK_a of about 10.5, indicating that at physiological pH LacY is protonated. There are several irreplaceable amino acid side chains involved in sugar binding and/or H$^+$ translocation that may be responsible for the alkaline pK_a. However, as revealed by the studies presented here, the pK_a cannot be assigned to a single amino acid side chain in this group.
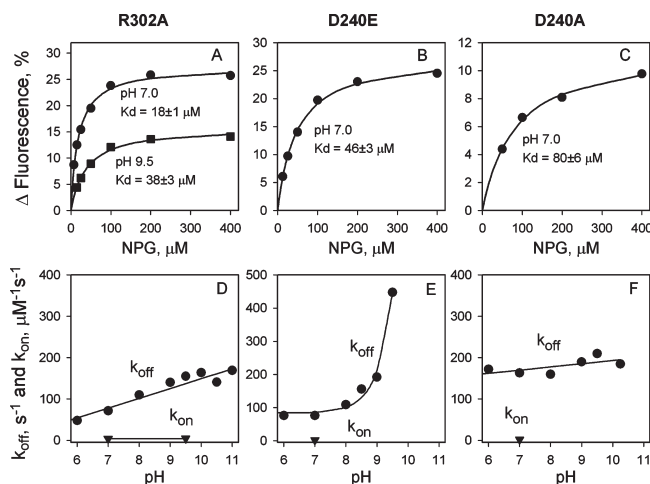
FIGURE 9: Kinetics of displacement of bound NPG by the excess of TDG: data for mutants R302A, D240E, and D240A. Upper panels: Dependence of amplitude of fluorescence changes on NPG concentrations at different pHs. Solid lines are hyperbolic fits to the data. Calculated K_d values at each pH are indicated. Lower panels: pH dependencies of measured displacement rates (k_{off}) and k_{on} calculated from K_d are presented as circles and triangles, respectively.

Although conservative replacement of the side chains directly involved in sugar binding greatly decreases affinity, each replacement exhibits the same pH dependence for TDG affinity as wild-type LacY (Figure 2). Furthermore, Arg302, Tyr236, His322, and Asp240, which do not make direct contact with the galacto-pyranosyl ring (*17*), are important for affinity nonetheless, because all replacements markedly increase K_d (Figure 3; Table 1). The conservative mutations R302K or Y236W cause acidic shifts in pK_a by ca. 2 pH units (Figure 3A,C). Replacements of Tyr236 with nonaromatic amino acids also cause an acid shift in pK_a (Figure 3D). However, Y236F or Y236K, as well as uncharged replacements for Arg302 or Asp240 and all replacements for His322, exhibit low-affinity TDG binding that is largely independent of pH (Figure 3; Table 1). These results indicate that protonation of individual amino acid residues does not determine pK_a for sugar-binding affinity in LacY, unlike in the case of KcsA channel where a clear effect of selected mutations in the H$^+$ binding cluster on pH sensitivity is observed (*50*).

Remarkably, neutral replacements for either Glu325 or Lys319 result in high-affinity galactoside binding over the entire pH range tested (Table 1; Figure 4; Figure 6B,C; Figure 7A−C; Figure 8). In contrast, conservative replacements at these positions exhibit decreased affinity, but pH dependencies are similar to wild-type LacY. Uncharged side chain replacements at positions 325 (*29, 44, 45, 48, 49*) or 319 (*46*) block all reactions that require net H$^+$ translocation with little or no effect on equilibrium exchange or counterflow. Pre-steady-state kinetic analysis indicates that the rate of sugar release rises sharply at alkaline pH with wild-type LacY, while it remains practically constant in the pH range 6−11 with uncharged mutants of Glu325 or Lys319. Therefore, the pH dependence of sugar affinity is determined by the k_{off} value, since k_{on} remains constant for wild-type LacY and the mutants studied. Notably, similar studies on the H$^+$-coupled multidrug antiporter EmrE indicate that the k_{off} for tetraphenylphosphonium does not depend on pH, while k_{on} increases markedly at alkaline pH so that affinity increases dramatically (K_d decreases) (*51*). In other words, the effects of pH on substrate binding kinetic parameters of EmrE are exactly opposite from those observed with LacY.
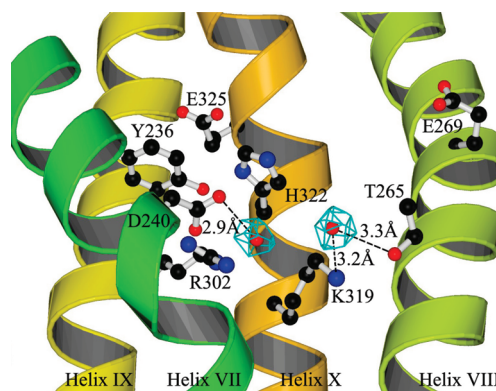

FIGURE 10: Water molecules in the H$^+$ translocation site of the refined LacY structure. Side view shown from the cytoplasmic cavity toward the H$^+$ translocation site. Residues important for H$^+$ translocation are displayed as balls and sticks, and water molecules are presented as red balls surrounded by globular densities in mesh presentation (shown with 2σ contour level). H-bonds between waters and amino acid residues are drawn as broken lines with distances in Å. See Supporting Information Refinement of LacY Structure for details. Illustration prepared using BobScript and Raster3D (*56, 57*).

The residues involved in H$^+$ translocation in LacY do not form a pathway through the membrane (Figure 1) (*9*). Rather Arg302, His322, Tyr236, and Asp240 form a tightly interconnected H-bond/salt bridge cluster in the middle of the molecule with Glu325 and Lys319 within 5 Å on opposite sides (Figure 1C). Any disturbance in the central core of the H$^+$ translocation site decreases sugar affinity by affecting H$^+$ binding, while uncharged side chains at positions 325 or 319 prevent H$^+$ escape from the cluster and maintain coupling with the sugar-binding site that retains high affinity even at very alkaline pH. Since no single amino acid residue in the central cluster of Arg302, His322, Tyr236, and Asp240 can be identified as an individual H$^+$ acceptor, perhaps coordinated water molecules within the H$^+$ binding site form a hydronium ion intermediate that cannot be deprotonated with neutral replacements for Lys319 or Glu325. By this means, water may behave like a cofactor in H$^+$ translocation.

Such a notion may also explain the phenotypes of the mutants in the H$^+$ translocation site. Mutants with neutral replacements for Glu325 or Lys319 catalyze equilibrium exchange and counterflow because LacY remains protonated, while replacement of the other side chains in the H-bond/salt bridge cluster results in loss of coordinated water molecule(s) so that LacY protonation and coupled sugar binding are impaired. Involvement of hydronium ions in H$^+$ binding and translocation was proposed originally by Boyer for F$_1$/F$_o$-ATPase (*52*) and used recently by von Ballmoos and Dimroth (*53*) to explain the unexpectedly high pK_a for the conserved carboxylic acid in the C subunit of the enzyme. Structural water molecules coordinating H$^+$ within the hydrophobic core of bacteriorhodopsin have also been identified (*54, 55*).

The electron density map of the amino acid residues involved in H$^+$ translocation is well-defined in all X-ray structures of LacY (*17−19*). Therefore, the structure of C154G LacY with the best overall resolution 2.95 Å (PDB ID 2cfq) (*18*) is reanalyzed here, and the refinements included additional reflections to 2.81 Å that were omitted originally (see Supporting Information Refinement of LacY Structure for details). There are two strong globular densities within the H$^+$ binding site in the composite omit map (over 5σ contour level) consistent with single water

molecules (Figure 10). One water molecule forms an H-bond with Asp240 and another with Lys319 and Thr265 (Figure 10, broken lines). These structural water molecules liganded by residues in the H^+ binding site may be important as hydronium ion intermediates during sugar/H^+ symport. Moreover, Thr265 is located in helix VIII one turn from irreplaceable Glu269, so that the water molecule connecting Lys319 and Thr265 may participate in the coupling between protonation and sugar binding.

ACKNOWLEDGMENT

SUPPORTING INFORMATION AVAILABLE

(1) Five figures showing steady-state TDG titrations at different pHs for all MIANS- or DACM-labeled LacY mutants and fitting curves used for the K_d^{app} estimation; (2) an example of pK_a value determination from dependencies of K_d^{app} on H^+ concentration presented for MIANS-labeled LacY mutants R302K and Y236W; (3) lactose transport data for D240N and K319Q mutants of LacY; (4) the details describing presented refinement of LacY structure. This material is available free of charge via the Internet at http://pubs.acs.org.

REFERENCES

1. Saier, M. H., Jr., Beatty, J. T., Goffeau, A., Harley, K. T., Heijne, W. H., Huang, S. C., Jack, D. L., Jahn, P. S., Lew, K., Liu, J., Pao, S. S., Paulsen, I. T., Tseng, T. T., and Virk, P. S. (1999) The major facilitator superfamily. *J. Mol. Microbiol. Biotechnol. 1*, 257–279.
2. Saier, M. H., Jr. (2000) Families of transmembrane sugar transport proteins. *Mol. Microbiol. 35*, 699–710.
3. West, I. C. (1970) Lactose transport coupled to proton movements in *Escherichia coli. Biochem. Biophys. Res. Commun. 41*, 655–661.
4. West, I. C., and Mitchell, P. (1973) Stoichiometry of lactose-H^+ symport across the plasma membrane of *Escherichia coli. Biochem. J.,* 132.
5. Foster, D. L., Garcia, M. L., Newman, M. J., Patel, L., and Kaback, H. R. (1982) Lactose-proton symport by purified *lac* carrier protein. *Biochemistry 21*, 5634–5638.
6. Kaback, H. R. (1983) The *lac* carrier protein in *Escherichia coli*: From membrane to molecule. *J. Membr. Biol. 76*, 95–112.
7. Kaback, H. R., Sahin-Toth, M., and Weinglass, A. B. (2001) The kamikaze approach to membrane transport. *Nat. Rev. Mol. Cell. Biol. 2*, 610–620.
8. Kaback, H. R. (2005) Structure and mechanism of the lactose permease. *C. R. Biol. 328*, 557–567.
9. Guan, L., and Kaback, H. R. (2006) Lessons from lactose permease. *Annu. Rev. Biophys. Biomol. Struct. 35*, 67–91.
10. Garcia, M. L., Viitanen, P., Foster, D. L., and Kaback, H. R. (1983) Mechanism of lactose translocation in proteoliposomes reconstituted with *lac* carrier protein purified from *Escherichia coli*. 1. Effect of pH and imposed membrane potential on efflux, exchange, and counterflow. *Biochemistry 22*, 2524–2531.
11. Kaczorowski, G. J., Robertson, D. E., and Kaback, H. R. (1979) Mechanism of lactose translocation in membrane vesicles from *Escherichia coli*. 2. Effect of imposed delta psi, delta pH, and delta mu H^+. *Biochemistry 18*, 3697–3704.
12. Zilberstein, D., Schuldiner, S., and Padan, E. (1979) Proton electrochemical gradient in *Escherichia coli* cells and its relation to active transport of lactose. *Biochemistry 18*, 669–673.
13. Patel, L., Garcia, M. L., and Kaback, H. R. (1982) Direct measurement of lactose/proton symport in *Escherichia coli* membrane vesicles: Further evidence for the involvement of histidine residue(s). *Biochemistry 21*, 5805–5810.
14. Frillingos, S., Sahin-Toth, M., Wu, J., and Kaback, H. R. (1998) Cys-scanning mutagenesis: A novel approach to structure function relationships in polytopic membrane proteins. *FASEB J. 12*, 1281–1299.
15. Guan, L., Hu, Y., and Kaback, H. R. (2003) Aromatic stacking in the sugar binding site of the lactose permease. *Biochemistry 42*, 1377–1382.
16. Vazquez-Ibar, J. L., Guan, L., Weinglass, A. B., Verner, G., Gordillo, R., and Kaback, H. R. (2004) Sugar recognition by the lactose permease of *Escherichia coli. J. Biol. Chem. 279*, 49214–49221.
17. Abramson, J., Smirnova, I., Kasho, V., Verner, G., Kaback, H. R., and Iwata, S. (2003) Structure and mechanism of the lactose permease of *Escherichia coli. Science 301*, 610–615.
18. Mirza, O., Guan, L., Verner, G., Iwata, S., and Kaback, H. R. (2006) Structural evidence for induced fit and a mechanism for sugar/H(+) symport in LacY. *EMBO J. 25*, 1177–1183.
19. Guan, L., Mirza, O., Verner, G., Iwata, S., and Kaback, H. R. (2007) Structural determination of wild-type lactose permease. *Proc. Natl. Acad. Sci. U.S.A. 104*, 15294–15298.
20. Dunten, R. L., Sahin-Tóth, M., and Kaback, H. R. (1993) Role of the charge pair formed by aspartic acid 237 and lysine 358 in the lactose permease of *Escherichia coli. Biochemistry 32*, 3139–3145.
21. Frillingos, S., Sahin-Tóth, M., Lengeler, J. W., and Kaback, H. R. (1995) Helix packing in the sucrose permease of *Escherichia coli*: Properties of engineered charge pairs between helices VII and XI. *Biochemistry 34*, 9368–9373.
22. He, M. M., Voss, J., Hubbell, W. L., and Kaback, H. R. (1995) Use of designed metal-binding sites to study helix proximity in the lactose permease of *Escherichia coli*. 1. Proximity of helix VII (Asp237 and Asp240) with helices X (Lys319) and XI (Lys358). *Biochemistry 34*, 15661–15666.
23. Abramson, J., Smirnova, I., Kasho, V., Verner, G., Iwata, S., and Kaback, H. R. (2003) The lactose permease of *Escherichia coli*: Overall structure, the sugar-binding site and the alternating access model for transport. *FEBS Lett. 555*, 96–101.
24. Kaback, H. R., Dunten, R., Frillingos, S., Venkatesan, P., Kwaw, I., Zhang, W., and Ermolova, N. (2007) Site-directed alkylation and the alternating access model for LacY. *Proc. Natl. Acad. Sci. U.S.A. 104*, 16504–16509.
25. Majumdar, D. S., Smirnova, I., Kasho, V., Nir, E., Kong, X., Weiss, S., and Kaback, H. R. (2007) Single-molecule FRET reveals sugar-induced conformational dynamics in LacY. *Proc. Natl. Acad. Sci. U.S.A. 104*, 12640–12645.
26. Smirnova, I., Kasho, V., Choe, J. Y., Altenbach, C., Hubbell, W. L., and Kaback, H. R. (2007) Sugar binding induces an outward facing conformation of LacY. *Proc. Natl. Acad. Sci. U.S.A. 104*, 16504–16509.
27. Zhou, Y., Guan, L., Freites, J. A., and Kaback, H. R. (2008) Opening and closing of the periplasmic gate in lactose permease. *Proc. Natl. Acad. Sci. U.S.A. 105*, 3774–3778.
28. Yamato, I., and Rosenbusch, J. P. (1983) Dependence on pH of substrate binding to lactose carrier in *Escherichia coli* cytoplasmic membranes. *FEBS Lett. 151*, 102–104.
29. Sahin-Tóth, M., Karlin, A., and Kaback, H. R. (2000) Unraveling the mechanism of lactose permease of *Escherichia coli. Proc. Natl. Acad. Sci. U.S.A. 97*, 10729–10732.
30. Smirnova, I. N., Kasho, V., and Kaback, H. R. (2008) Protonation and sugar binding to LacY. *Proc. Natl. Acad. Sci. U.S.A. 105*, 8896–8901.
31. Fitch, C. A., Karp, D. A., Lee, K. K., Stites, W. E., Lattman, E. E., and Garcia-Moreno, E. B. (2002) Experimental pK(a) values of buried residues: Analysis with continuum methods and role of water penetration. *Biophys. J. 82*, 3289–3304.
32. Baran, K. L., Chimenti, M. S., Schlessman, J. L., Fitch, C. A., Herbst, K. J., and Garcia-Moreno, B. E. (2008) Electrostatic effects in a network of polar and ionizable groups in staphylococcal nuclease. *J. Mol. Biol. 379*, 1045–1062.
33. He, M., and Kaback, H. R. (1997) Interaction between residues Glu269 (helix VIII) and His322 (helix X) of the lactose permease of *Escherichia coli* is essential for substrate binding. *Biochemistry 36*, 13688–13692.
34. Smirnova, I. N., Kasho, V. N., and Kaback, H. R. (2006) Direct sugar binding to LacY measured by resonance energy transfer. *Biochemistry 45*, 15279–15287.
35. Weinglass, A. B., Smirnova, I. N., and Kaback, H. R. (2001) Engineering conformational flexibility in the lactose permease of *Escherichia coli*: Use of glycine-scanning mutagenesis to rescue mutant Glu325→Asp. *Biochemistry 40*, 769–776.
36. Sahin-Tóth, M., le Coutre, J., Kharabi, D., le Maire, G., Lee, J. C., and Kaback, H. R. (1999) Characterization of Glu126 and Arg144, two residues that are indispensable for substrate binding in the lactose permease of *Escherichia coli. Biochemistry 38*, 813–819.

37. Venkatesan, P., and Kaback, H. R. (1998) The substrate-binding site in the lactose permease of *Escherichia coli. Proc. Natl. Acad. Sci. U.S.A. 95*, 9802–9807.

38. Weinglass, A. B., Whitelegge, J. P., Hu, Y., Verner, G. E., Faull, K. F., and Kaback, H. R. (2003) Elucidation of substrate binding interactions in a membrane transport protein by mass spectrometry. *EMBO J. 22*, 1467–1477.

39. Klauda, J. B., and Brooks, B. R. (2007) Sugar binding in lactose permease: Anomeric state of a disaccharide influences binding structure. *J. Mol. Biol. 367*, 1523–1534.

40. Menick, D. R., Sarkar, H. K., Poonian, M. S., and Kaback, H. R. (1985) Cys154 is important for *lac* permease activity in *Escherichia coli. Biochem. Biophys. Res. Commun. 132*, 162–170.

41. Smirnova, I. N., and Kaback, H. R. (2003) A mutation in the lactose permease of *Escherichia coli* that decreases conformational flexibility and increases protein stability. *Biochemistry 42*, 3025–3031.

42. Nie, Y., Sabetfard, F. E., and Kaback, H. R. (2008) The Cys154→Gly mutation in LacY causes constitutive opening of the hydrophilic periplasmic pathway. *J. Mol. Biol. 379*, 695–703.

43. Kasho, V. N., Smirnova, I. N., and Kaback, H. R. (2006) Sequence alignment and homology threading reveals prokaryotic and eukaryotic proteins similar to lactose permease. *J. Mol. Biol. 358*, 1060–1070.

44. Carrasco, N., Antes, L. M., Poonian, M. S., and Kaback, H. R. (1986) *Lac* permease of *Escherichia coli*: Histidine-322 and glutamic acid-325 may be components of a charge-relay system. *Biochemistry 25*, 4486–4488.

45. Carrasco, N., Puttner, I. B., Antes, L. M., Lee, J. A., Larigan, J. D., Lolkema, J. S., Roepe, P. D., and Kaback, H. R. (1989) Characterization of site-directed mutants in the *lac* permease of *Escherichia coli*. 2. Glutamate-325 replacements. *Biochemistry 28*, 2533–2539.

46. Persson, B., Roepe, P. D., Patel, L., Lee, J., and Kaback, H. R. (1992) Site-directed mutagenesis of lysine 319 in the lactose permease of *Escherichia coli. Biochemistry 31*, 8892–8897.

47. Sahin-Tóth, M., and Kaback, H. R. (1993) Properties of interacting aspartic acid and lysine residues in the lactose permease of *Escherichia coli. Biochemistry 32*, 10027–10035.

48. Franco, P. J., and Brooker, R. J. (1994) Functional roles of Glu-269 and Glu-325 within the lactose permease of *Escherichia coli. J. Biol. Chem. 269*, 7379–7386.

49. Sahin-Tóth, M., and Kaback, H. R. (2001) Arg-302 facilitates deprotonation of Glu-325 in the transport mechanism of the lactose permease from *Escherichia coli. Proc. Natl. Acad. Sci. U.S.A. 98*, 6068–6073.

50. Thompson, A. N., Posson, D. J., Parsa, P. V., and Nimigean, C. M. (2008) Molecular mechanism of pH sensing in KcsA potassium channels. *Proc. Natl. Acad. Sci. U.S.A. 105*, 6900–6905.

51. Adam, Y., Tayer, N., Rotem, D., Schreiber, G., and Schuldiner, S. (2007) The fast release of sticky protons: kinetics of substrate binding and proton release in a multidrug transporter. *Proc. Natl. Acad. Sci. U.S.A. 104*, 17989–17994.

52. Boyer, P. D. (1988) Bioenergetic coupling to protonmotive force: Should we be considering hydronium ion coordination and not group protonation? *Trends Biochem. Sci. 13*, 5–7.

53. von Ballmoos, C., and Dimroth, P. (2007) Two distinct proton binding sites in the ATP synthase family. *Biochemistry 46*, 11800–11809.

54. Garczarek, F., Brown, L. S., Lanyi, J. K., and Gerwert, K. (2005) Proton binding within a membrane protein by a protonated water cluster. *Proc. Natl. Acad. Sci. U.S.A. 102*, 3633–3638.

55. Garczarek, F., and Gerwert, K. (2006) Functional waters in intra-protein proton transfer monitored by FTIR difference spectroscopy. *Nature 439*, 109–112.

56. Esnouf, R. M. (1999) Further additions to MolScript version 1.4, including reading and contouring of electron-density maps. *Acta Crystallogr., Sect. D: Biol. Crystallogr. 55*, 938–940.

57. Merritt, E. A., and Bacon, D. J. (1977) Raster3D: Photorealistic molecular graphics. *Methods Enzymol. 277*, 504–524.